



TITLE:

Impact of P-glycoprotein and breast cancer resistance protein on the brain distribution of antiepileptic drugs in knockout mouse models.

AUTHOR(S):

Nakanishi, Haruka; Yonezawa, Atsushi; Matsubara, Kazuo; Yano, Ikuko

CITATION:

Nakanishi, Haruka ...[et al]. Impact of P-glycoprotein and breast cancer resistance protein on the brain distribution of antiepileptic drugs in knockout mouse models.. European journal of pharmacology 2013, 710(1-3): 20-28

ISSUE DATE:

2013-06-15

URL:

<http://hdl.handle.net/2433/175253>

RIGHT:

© 2013 Elsevier B.V.; This is not the published version. Please cite only the published version.; この論文は出版社版ではありません。引用の際には出版社版をご確認ご利用ください。

Impact of P-glycoprotein and breast cancer resistance protein on the brain distribution of antiepileptic drugs in knockout mouse models

Haruka Nakanishi^a, Atsushi Yonezawa^b, Kazuo Matsubara^b, and Ikuko Yano^{a,*}

^aDepartment of Clinical Pharmacy and Education, Graduate School of Pharmaceutical Sciences,
Kyoto University, Kyoto 606-8501, Japan

^bDepartment of Pharmacy, Kyoto University Hospital, Kyoto 606-8507, Japan

*Corresponding author: Ikuko Yano, Ph.D.

Department of Clinical Pharmacy and Education

Graduate School of Pharmaceutical Sciences, Kyoto University

Sakyo-ku, Kyoto 606-8501, Japan

Tel: +81-75-751-3582

Fax: +81-75-751-3205

E-mail: iyano@kuhp.kyoto-u.ac.jp

Abstract

Refractory epilepsy is reportedly associated with an overexpression of ATP-binding cassette transporters such as P-glycoprotein (Pgp) and breast cancer resistance protein (Bcrp). In this study, we examined the contribution of Pgp and Bcrp to the brain distribution of 12 antiepileptic drugs (AEDs) in *Mdr1a/1b(-/-)* and *Mdr1a/1b(-/-)/Bcrp(-/-)* mice within a therapeutic concentration range. The blood concentrations were sequentially determined, and the brain concentrations were measured at 60 min after intravenous administration. The plasma concentration profiles for each AED in the *Mdr1a/1b(-/-)* mice were equivalent to those in the wild-type mice. In contrast, the plasma concentration profiles of phenytoin, lamotrigine, topiramate, tiagabine, and levetiracetam in the *Mdr1a/1b(-/-)/Bcrp(-/-)* mice were significantly lower than the corresponding ones in the wild-type mice. The brain-to-plasma concentration ratio ($K_{p_{\text{brain}}}$) values of phenytoin, topiramate, and tiagabine in the *Mdr1a/1b(-/-)* mice were significantly higher than the corresponding ones in the wild-type mice. In contrast, the $K_{p_{\text{brain}}}$ values of phenobarbital, clobazam, zonisamide, gabapentin, tiagabine, and levetiracetam in the *Mdr1a/1b(-/-)/Bcrp(-/-)* mice were significantly higher than the corresponding ones in *Mdr1a/1b(-/-)* mice. The $K_{p_{\text{brain}}}$ values of the 12 AEDs in the *Mdr1a/1b(-/-)/Bcrp(-/-)* mice, but not wild-type mice, significantly correlated with the corresponding molecular weight values. These findings suggest that both Pgp and Bcrp restrict brain access for several AEDs. Taken together, information on the contribution of each transporter may be useful in the development of strategic treatments of refractory epilepsy.

Keywords: antiepileptic drug; Abcb1; Abcg2; blood-brain barrier; knockout mice; pharmacokinetics

1. Introduction

Epilepsy is the most prevalent chronic neurological disorder, and it affects at least 50 million people worldwide (Kwan et al., 2011). After the 1990s, a new generation of antiepileptic drugs (AEDs) emerged and more than 20 AEDs have been clinically used worldwide. The majority of epilepsy patients have good control over their seizures with AED use; however, approximately 30% of epilepsy patients exhibit refractory epilepsy, which is characterized by uncontrolled seizures, despite multiple AED treatments (Gao et al., 2012; Kwan et al., 2010). These epilepsy patients are often resistant to a range of AEDs, although these drugs differ from each other in their pharmacokinetic properties and mechanisms of action.

ATP-binding cassette (ABC) transporters, including P-glycoprotein (Pgp; also known as Mdr1; Abcb1), multidrug resistance-associated proteins (Mrps; Abccs), and breast cancer resistance protein (Bcrp; Abcg2), are transmembrane proteins that function in the disposition of a wide variety of drugs (Löscher and Potschka, 2005). Most multidrug ABC transporters have broad and substantially overlapping substrate specificities, and their substrates include many drugs and drug metabolites (Lagas et al., 2009). It has been hypothesized that the overexpression of ABC transporters at the blood-brain barrier (BBB) contributes to drug resistance. The expression of Pgp

and Bcrp has been shown to be up-regulated in brain capillary endothelial cells in epilepsy patients or animal models of epilepsy (Aronica et al., 2005; Dombrowski et al., 2001; van Vliet et al., 2005).

The transporter hypothesis is based on the assumption that many or almost all AEDs are substrates of ABC transporters. In the recent review (Zang et al., 2012), many AEDs have been classified into five categories on the Pgp substrate status combining the evidence of *in vitro* cell models and *in vivo* animal models or patients. For example, phenytoin and carbamazepine have been widely used to treat several types of epilepsy for many decades, and they were suggested to be definite and possible substrates for Pgp, respectively (Zhang et al., 2012). Although *in vitro* evidence on the Pgp status of AEDs using the Pgp-expressing cell models was accumulated, evidence from animal models is not fully available (Zhang et al., 2012; Löscher et al., 2011). In addition, limited information is available regarding the interaction between Bcrp and AEDs (Cerveny et al., 2006).

The purpose of this study was to assess the effects of Pgp and Bcrp on the brain distribution of 12 AEDs in *Mdr1a/1b*(-/-) and *Mdr1a/1b*(-/-)/*Bcrp*(-/-) mice. In this study, we simultaneously administered 6 AEDs within a therapeutic concentration range and measured the drug concentrations using ultra-performance liquid chromatography combined with tandem mass spectrometry (UPLC-MS/MS), which helps evaluate the characteristics of each drug and minimizes

the effects of inter-individual variability and experimental errors.

2. Materials and Methods

2.1. Materials

Carbamazepine, phenobarbital sodium, phenytoin, valproate sodium, and zonisamide were purchased from Wako Pure Chemical Industries Ltd. (Osaka, Japan). Ethosuximide, gabapentin, topiramate, tiagabine, and levetiracetam were purchased from Toronto Research Chemical Inc. (North York, ON, Canada). Lamotrigine was purchased from LKT Laboratories, Inc. (St. Paul, MN, USA). Clobazam was a gift from Dainippon Sumitomo Pharma Co., Ltd. (Osaka, Japan). All other chemicals used were of the highest grade available. The chemical structures of all of the investigated AEDs are shown in Fig. 1.

2.2. Animals

Male *Mdr1a/1b*(-/-) and *Mdr1a/1b*(-/-)/*Bcrp*(-/-) mice obtained from Taconic Farms (Germantown, NY, USA) and male wild-type mice of the same genetic background (FVB) obtained from CLEA Japan (Yokohama, Japan) between the ages of 9 and 16 weeks were used. The animals were anesthetized with isoflurane (inhalation) (anesthesia system of animal; DS Pharma Biomedical Co., Ltd., Osaka, Japan), and the animal experiments were performed in accordance with the

Guidelines for Animal Experiments of Kyoto University.

2.3. Pharmacokinetics studies

The femoral and jugular veins were cannulated with polyethylene tubing for drug administration (PE-10; BD Biosciences, San Jose, CA, USA) and blood sampling (SP31; Natsume Seisakusho Co. Ltd., Tokyo, Japan), respectively. The 12 AEDs were divided into 2 groups: (1) phenytoin (10 mg/kg), carbamazepine (10 mg/kg), gabapentin (10 mg/kg), lamotrigine (3 mg/kg), topiramate (10 mg/kg), and levetiracetam (10 mg/kg), and (2) phenobarbital (5 mg/kg), ethosuximide (50 mg/kg), valproic acid (50 mg/kg), clobazam (0.5 mg/kg), zonisamide (5 mg/kg), and tiagabine (0.5 mg/kg). Each dosage was determined so that the plasma concentrations were within the therapeutic range. Each group of AEDs was dissolved in saline containing 10% ethanol and 10% Cremophor[®] EL (Nacalai Tesque, Inc., Kyoto, Japan). The solution for the first group was alkalinized for phenytoin. The AEDs-mixture solutions were then intravenously injected at a volume of 10 mL/kg via the catheterized femoral vein over 3 min at the beginning of the time course. Blood samples (0.05–0.07 mL) were collected from the jugular vein at 5, 10, 15, 30, and 60 min after the injection. Plasma was immediately separated by centrifugation (20,238 g for 5 min at

room temperature), and stored at -20°C until assayed. After 60 min, the whole brain, kidney, and liver were removed and homogenized in either an equal (brain) volume of or 4 times (kidney and liver) the volume of saline. Homogenized tissues were centrifuged (21,800 g for 5 min at 4°C), and the supernatant was stored at -20°C until further assayed.

The concentrations of the 12 AEDs in the plasma and tissues were measured using UPLC-MS/MS (Waters Corporation, Milford, MA, USA) as previously described (Shibata et al., 2012).

2.4. Data analysis

The pharmacokinetic parameters, total body clearance (CL), volume of distribution at steady state (V_{ss}), and terminal half-life ($T_{1/2}$) were calculated by non-compartmental analysis with WinNonlin[®] version 6.0 (Pharsight, Sunnyvale, CA, USA). The tissue distribution of each AED in the mice was evaluated using the tissue-to-plasma concentration ratio ($K_{p\text{tissue}}$) at 60 min after administration.

To determine the covariate of $K_{p\text{brain}}$, we examined the regression between the $K_{p\text{brain}}$ values in the *Mdr1a/1b*(-/-)/*Bcrp*(-/-) mice and the molecular weight (MW) or logarithm of the calculated

partition coefficient (cLogP):

$$Kp_{\text{brain}} = \theta_1 + \theta_2 \times \text{cLogP} + \theta_3 \times \text{MW}^{\theta_4}$$

where θ_1 – θ_4 are the mean estimated parameters. The MW and cLogP of the 12 AEDs were calculated using ChemDraw[®] version 12.0 (PerkinElmer Inc., Waltham, MA, USA), and model analyses were performed using the nonlinear mixed-effects modeling program NONMEM version 7.2 (Beal et al., 1992). The effect of the MW and cLogP was examined using the smallest Akaike information criterion (AIC) values (Akaike, 1974).

The values were expressed as means \pm S.E. The statistical software package GraphPad Prism[®] version 5.0 (GraphPad Software, Inc., San Diego, CA, USA) were used for performing statistical analyses. The plasma concentration profiles were compared by repeated measures analysis of variance (ANOVA). The statistical differences between the mean values were analyzed using the non-paired *t*-test if the variance was equivalent. If the variance was not equivalent, then the Mann-Whitney test was performed. Multiple comparisons were performed using ANOVA followed by the Bonferroni test. The Pearson's correlation coefficient (*r*) was used to estimate the correlations between 2 factors. A value of $P < 0.05$ was considered to be statistically significant.

3. Results

3.1. Pharmacokinetics of 12 AEDs in the wild-type, *Mdr1a/1b*(-/-), and *Mdr1a/1b*(-/-)/*Bcrp*(-/-) mice

The plasma concentration profiles of all of the 12 AEDs were similar between the *Mdr1a/1b*(-/-) mice and wild-type mice (Fig. 2). In contrast, the plasma concentration profiles of phenytoin, lamotrigine, topiramate, tiagabine, and levetiracetam were found to be decreased in the *Mdr1a/1b*(-/-)/*Bcrp*(-/-) mice compared to wild-type mice (Fig. 3). The pharmacokinetic parameters of the 12 AEDs in the *Mdr1a/1b*(-/-) and *Mdr1a/1b*(-/-)/*Bcrp*(-/-) mice are summarized in Tables 1 and 2, respectively. The CL, V_{ss} , and $T_{1/2,\lambda}$ of each AED in the *Mdr1a/1b*(-/-) mice were comparable to those in the wild-type mice. In contrast, the CL of zonisamide, gabapentin, and levetiracetam was significantly higher in the *Mdr1a/1b*(-/-)/*Bcrp*(-/-) mice than in the wild-type mice, and the V_{ss} of phenytoin, clobazam, topiramate, and levetiracetam were found to be significantly increased in the *Mdr1a/1b*(-/-)/*Bcrp*(-/-) mice compared to the wild-type mice. The $T_{1/2,\lambda}$ of zonisamide and levetiracetam were smaller in the *Mdr1a/1b*(-/-)/*Bcrp*(-/-) mice than in the wild-type mice.

3.2. Impact of Pgp and Bcrp on AED tissue distribution

The brain-to-plasma concentration ratio ($K_{p_{\text{brain}}}$) values of the 12 AEDs examined at 60 min are shown as the percentage of the control (wild-type mice) (Fig. 4). The $K_{p_{\text{brain}}}$ values of phenytoin, topiramate, and tiagabine were found to be significantly increased (1.44-, 1.50-, and 1.31-fold, respectively) in the *Mdr1a/1b*(-/-) mice compared to the wild-type mice. In contrast, the $K_{p_{\text{brain}}}$ values of phenobarbital, clobazam, zonisamide, gabapentin, tiagabine, and levetiracetam were significantly higher (1.49-, 1.33-, 1.17-, 1.61-, 1.49-, and 1.28-fold, respectively) in the *Mdr1a/1b*(-/-)/*Bcrp*(-/-) mice than in the *Mdr1a/1b*(-/-) mice.

The kidney or liver-to-plasma concentration ratios ($K_{p_{\text{kidney}}}$ and $K_{p_{\text{liver}}}$, respectively) in the *Mdr1a/1b*(-/-) and *Mdr1a/1b*(-/-)/*Bcrp*(-/-) mice are summarized in Tables 1 and 2, respectively. In each strain, the $K_{p_{\text{liver}}}$ values for all AEDs were in the range of 0.633–2.36. The $K_{p_{\text{liver}}}$ value of gabapentin was found to be significantly decreased in the *Mdr1a/1b*(-/-) mice, and the $K_{p_{\text{liver}}}$ value of lamotrigine was found to be significantly increased in the *Mdr1a/1b*(-/-)/*Bcrp*(-/-) mice compared to the wild-type mice. The $K_{p_{\text{kidney}}}$ values were in the range of 0.558–2.24, except that of gabapentin, which was in the range of 3.27–5.52. In the *Mdr1a/1b*(-/-) mice, the $K_{p_{\text{kidney}}}$ value of valproic acid was significantly decreased. In contrast, compared to the wild-type mice, the

Mdr1a/1b(-/-) mice showed significantly increased Kp_{kidney} value of clobazam. Furthermore, in the *Mdr1a/1b(-/-)/Bcrp(-/-)* mice, the Kp_{kidney} values of phenytoin, carbamazepine, and topiramate were significantly higher, and the Kp_{kidney} value for gabapentin was significantly lower than the corresponding values in the wild-type mice.

3.3. Relationship between the Kp_{brain} value and MW or cLogP

After using the backward elimination and forward inclusion method, we selected the final model using the smallest AIC value in the *Mdr1a/1b(-/-)/Bcrp(-/-)* mice:

$$Kp_{\text{brain}} (\textit{Mdr1a/1b(-/-)/Bcrp(-/-)} \text{ mice}) = 0.00304 \times \text{MW}$$

The relationship between the Kp_{brain} value and MW in the wild-type mice, and the Kp_{kidney} and Kp_{liver} values in both strains were also examined, and are shown in Fig. 5. The Kp_{brain} value in the wild-type mice did not correlate with either the MW or cLogP. Furthermore, the Kp_{kidney} value did not correlate with either the MW in the *Mdr1a/1b(-/-)/Bcrp(-/-)* or wild-type mice. However, the Kp_{liver} value showed a significant relationship with the MW in both the *Mdr1a/1b(-/-)/Bcrp(-/-)* and wild-type mice.

4. Discussion

Our study demonstrated 2 main findings: (a) Pgp contributed to the limitation of the brain distribution of phenytoin, topiramate, and tiagabine, and (b) Bcrp participated in the restriction of the brain distribution of phenobarbital, clobazam, zonisamide, gabapentin, tiagabine, and levetiracetam.

In this study, phenytoin, topiramate, and tiagabine proved to be Pgp substrates, and ethosuximide, carbamazepine, valproic acid, and lamotrigine were not substrates. A previous *in vivo* study using *Mdr1a/1b*(-/-) mice showed a 46% increase in hippocampal phenytoin concentrations (Rizzi et al., 2002). In the same report, carbamazepine concentrations were measurable in the hippocampal in *Mdr1a/1b*(-/-) mice, whereas they were undetectable in wild-type mice (Rizzi et al., 2002). In another study, *Mdr1a/1b*(-/-) mice did not exhibit significantly different brain concentrations of carbamazepine after intraperitoneal administration from those in wild-type mice (Owen et al., 2001). Thus, phenytoin was evidenced as a Pgp substrate in several reports using *in vitro* and *in vivo* models, but carbamazepine status for Pgp substrate was controversial (Löscher et al., 2011; Zhang et al., 2012). Brain distribution of topiramate was higher in *Mdr1a* (-/-) mice than in wild-type controls (Sills et al., 2002), while ethosuximide was unlikely a Pgp substrate in the

Mdr1a/1b (-/-) mouse model (Doran et al., 2005). Therefore, our data were consistent with the previous results using *in vivo* *Mdr1* knockout mice for phenytoin, topiramate, and ethosuximide, and added the new information on the Pgp-substrate status for tiagabine, valproic acid, and lamotrigine.

In addition, we used *Mdr1a/1b*(-/-)/*Bcrp*(-/-) mice to evaluate the Pgp and Bcrp substrate status of AEDs. In the mouse BBB, the expression levels of Pgp were the highest of all the examined ABC transporters, and Pgp played a pivotal role in drug efflux from the brain (Hartz and Bauer, 2010). Moreover, multiple transporter gene knockout mouse models have been commonly used to elucidate the synergistic role of Pgp and Bcrp in the efflux of dual substrates at the BBB. Although several studies that compared *Bcrp*(-/-) and wild-type mice failed to demonstrate a function of Bcrp in the disposition of topotecan, a substrate of both Pgp and Bcrp, the comparison of the *Mdr1a/1b*(-/-)/*Bcrp*(-/-) mice and *Mdr1a/1b*(-/-) mice indicated a contribution of Bcrp to topotecan distribution in the brain (de Vries et al., 2007). As illustrated by the recent positron emission tomography data of verapamil (Bauer et al., 2012), the *Mdr1a/1b*(-/-)/*Bcrp*(-/-) mice showed much higher brain levels than would have been expected from data in either *Mdr1* or *Bcrp* knockout mice. Therefore, the *Mdr1a/1b*(-/-)/*Bcrp*(-/-) mouse model was powerful tool to

investigate the synergistic role of Pgp and Bcrp to the brain distribution of AEDs which are both Pgp and Bcrp substrates. In our study, we found that the $K_{p_{\text{brain}}}$ values of phenobarbital, clobazam, zonisamide, gabapentin, and levetiracetam increased in the *Mdr1a/1b*(-/-)/*Bcrp*(-/-) mice compared to the *Mdr1a/1b*(-/-) mice. Thus, these AEDs are substrates for Bcrp. However, these results may be attributable to the cooperative effects of Pgp and Bcrp, and we cannot exclude the potential contribution of Pgp to the brain efflux of these 5 AEDs. If we investigated the brain distribution of AEDs using *Bcrp*(-/-) mice, the information on the contribution of Pgp to the brain efflux of these AEDs may be obtained.

To the best of our knowledge, there have been no *in vivo* reports regarding the involvement of Bcrp in the restriction of AED distribution in the brain. The previous *in vitro* report using human Bcrp-expressing Madin-Darby canine kidney cells showed a lack of interaction between Bcrp and phenytoin, phenobarbital, ethosuximide, carbamazepine, valproic acid, and lamotrigine (Cerveny et al., 2006). In this study, the $K_{p_{\text{brain}}}$ value of phenobarbital was found to be significantly increased in the *Mdr1a/1b*(-/-)/*Bcrp*(-/-) mice compared to the *Mdr1a/1b*(-/-) mice (Fig. 4A), which was inconsistent with the result of a previous study (Cerveny et al., 2006). This discrepancy may be due to the differences in the *in vitro* experimental conditions or in species. This is exemplified in cells

that express human or mouse Pgp, where there are species differences in AED transport (Baltes et al., 2007). Since it is difficult to directly assess the drug distribution in the human brain, a combination of *in vitro* and *in vivo* data is important to predict AED brain access in humans. The plasma concentration profiles in phenytoin, lamotrigine, topiramate, tiagabine, and levetiracetam were found to be decreased in the *Mdr1a/1b(-)/Bcrp(-)* mice compared to the wild-type mice (Fig. 3). These alterations may be because of the restriction of drug distribution by both Pgp and Bcrp in the brain and/or other elimination organs.

There was a significant difference between the $K_{p\text{brain}}$ values of phenytoin in the wild-type and *Mdr1a/1b(-)* mice; however, there were no significant differences between the $K_{p\text{brain}}$ values of phenytoin in the wild-type and *Mdr1a/1b(-)/Bcrp(-)* mice (Fig. 4B). This discrepancy may be due to an experimental error; however, potential compensatory effects in the *Mdr1a/1b(-)/Bcrp(-)* mice should not be discounted. Namely, the expression of other transporters may be affected and consequently mask the genuine effects of Pgp or Bcrp. Phenytoin has been reported to be transported by Mrp2 (Potschka et al., 2003). Thus, the present results might be explained by the functional enhancement and/or increased expression level of Mrp2 at the BBB in the *Mdr1a/1b(-)/Bcrp(-)* mice, although a recent study using a quantitative proteomics approach

showed no compensatory changes in the BBB expression of several transporters (i.e., Pgp, Bcrp, and Mrps) in *Mdr1a/1b*(-/-), *Bcrp*(-/-) and *Mdr1a/1b*(-/-)/*Bcrp*(-/-) mice (Agarwal et al., 2012).

We found that the $K_{p_{\text{brain}}}$ values in the *Mdr1a/1b*(-/-)/*Bcrp*(-/-) mice significantly correlated with the MW values, and the $K_{p_{\text{liver}}}$ values also significantly correlated with the MW values in both the *Mdr1a/1b*(-/-)/*Bcrp*(-/-) and wild-type mice. However, no correlation was observed between the $K_{p_{\text{brain}}}$ and MW values in the wild-type mice. Since the $K_{p_{\text{liver}}}$ values of nearly all AEDs were unaffected in the *Mdr1a/1b*(-/-)/*Bcrp*(-/-) mice, the effects of Pgp and Bcrp on the liver distribution of many AEDs were considered to be negligible, and the distribution of the 12 AEDs were predicted from their MW values. Further, in case of a lack of contribution from Pgp and Bcrp at the BBB, brain distribution of many AEDs would depend on their MW values. Therefore, of the several ABC transporters in the BBB, Pgp and Bcrp appear to play a pivotal role in the efflux of AEDs from the brain. Since the observed $K_{p_{\text{brain}}}$ values of phenytoin and valproic acid were relatively lower than their predicted values, other efflux transporters might also affect the distribution of these AEDs in the brain (Fig. 5A). Furthermore, since the observed $K_{p_{\text{brain}}}$ values of ethosuximide, clobazam, and zonisamide were higher than their predicted values, these AEDs exhibited several properties that enabled effective distribution in the brain.

The $K_{p_{\text{brain}}}$ value of each AED in the *Mdr1a/1b*(-/-)/*Bcrp*(-/-) mice was at most 2-fold higher than that in the wild-type mice, which indicated that Pgp and Bcrp played a relatively minor role in the efflux of AEDs from the brain (Fig. 4). However, Pgp and Bcrp may have vital clinical roles, because these transporters were overexpressed in patients with refractory epilepsy (Aronica et al., 2005; Dombrowski et al., 2001). This is also supported by the higher expression levels of Bcrp in the human brain capillary endothelial cells than in mice (Uchida et al., 2011). Considering the effects of brain efflux transporters at the human BBB, information on the substrate status of Bcrp is valuable. Thus, additional clinical research is required to determine the proper selection of AEDs for the treatment of refractory epilepsy.

Our study had some restrictions that should be discussed. Since 6 AEDs were injected simultaneously, some pharmacokinetic drug-drug interactions might occur and affect the Pgp and Bcrp status of each AED. However, since combined AEDs are general in the treatment of refractory epilepsy, it is meaningful to investigate the brain distribution of each drug after the simultaneous administration in the therapeutic ranges. On one hand, Pgp-mediated transport was reported to highly depend on the AED concentrations (Löscher et al., 2011). Each AED was used at only one dose in this study, which may lead to false negative results. We tried to investigate the interaction of

AEDs with Pgp or Bcrp in the therapeutic concentration range in humans, but the concentrations of zonisamide and lamotrigine were below the therapeutic range, and that of tiagabine was above the range (Figs. 2 and 3). Our data showed that zonisamide was interacted with Bcrp, and that tiagabine was interacted with both Pgp and Bcrp. On one hand, Pgp or Bcrp-mediated brain distribution of lamotrigine was not apparent, although the plasma concentration profile of lamotrigine in the *Mdr1a/1b(-)/Bcrp(-)* mice were significantly lower than that in the wild-type mice. Brain access of lamotrigine was limited by Pgp in the *in vivo* brain microdialysis study in rats (Potschka et al., 2002). Since plasma concentrations of lamotrigine in their study were 2-fold higher than those in the present study, Pgp-mediated interaction may be identified if higher concentrations were used. In addition, only the whole brain was analysed at only one time point (60 min after the intravenous administration) in this study, which may lead to false negative results for the Pgp transport. More precise studies using the brain fraction and time course data were needed in the future

5. Conclusion

Taken together, the findings of the present study indicate that both Pgp and Bcrp significantly affect the brain distribution of several AEDs. Studies evaluating the contribution of each transporter may be useful in the development of strategic treatments of refractory epilepsy.

Acknowledgments

This work was partially supported by the Grant-in-Aid for Scientific Research from the Ministry of Education, Culture, Sports, Science and Technology of Japan.

References

- Agarwal, S., Uchida, Y., Mittapalli, R.K., Sane, R., Terasaki, T., Elmquist, W.F., 2012. Quantitative proteomics of transporter expression in brain capillary endothelial cells isolated from P-glycoprotein (P-gp), breast cancer resistance protein (Bcrp), and P-gp/Bcrp knockout mice. *Drug Metab. Dispos.* 40, 1164-1169.
- Akaike, H., 1974. A new look at statistical model identification. *IEEE Trans. Automat. Contr.* Ac-19, 716-723.
- Aronica, E., Gorter, J.A., Redeker, S., van Vliet, E.A., Ramkema, M., Scheffer, G.L., Scheper, R.J., van der Valk, P., Leenstra, S., Baayen, J.C., Spliet, W.G., Troost, D., 2005. Localization of breast cancer resistance protein (BCRP) in microvessel endothelium of human control and epileptic brain. *Epilepsia* 46, 849-857.
- Baltes, S., Gastens, A.M., Fedrowitz, M., Potschka, H., Kaever, V., Löscher, W., 2007. Differences in the transport of the antiepileptic drugs phenytoin, levetiracetam and carbamazepine by human and mouse P-glycoprotein. *Neuropharmacology* 52, 333-346.
- Bauer, F., Wanek, T., Mairinger, S., Stanek, J., Sauberer, M., Kuntner, C., Parveen, Z., Chiba, P.,

Müller, M., Langer, O., Erker, T., 2012. Interaction of HM30181 with P-glycoprotein at the murine blood-brain barrier assessed with positron emission tomography. *Eur J Pharmacol.* 696, 18-27.

Beal, S., Boeckmann, A., Sheiner, L., 1992. *NONMEM user's guides*. NONMEM Project Group, San Francisco, CA: University of California at San Francisco.

Cervený, L., Pavek, P., Malakova, J., Staud, F., Fendrich, Z., 2006. Lack of interactions between breast cancer resistance protein (BCRP/ABCG2) and selected antiepileptic agents. *Epilepsia* 47, 461-468.

de Vries, N.A., Zhao, J., Kroon, E., Buckle, T., Beijnen, J.H., van Tellingen, O., 2007. P-glycoprotein and breast cancer resistance protein: two dominant transporters working together in limiting the brain penetration of topotecan. *Clin. Cancer Res.* 13, 6440-6449.

Dombrowski, S.M., Desai, S.Y., Marroni, M., Cucullo, L., Goodrich, K., Bingaman, W., Mayberg, M.R., Benge, L., Janigro, D., 2001. Overexpression of multiple drug resistance genes in endothelial cells from patients with refractory epilepsy. *Epilepsia* 42, 1501-1506.

Doran, A., Obach, R.S., Smith, B.J., Hosea, N.A., Becker, S., Callegari, E., Chen, C., Chen, X., Choo, E., Cianfroga, J., et al. (2005) The impact of P-glycoprotein on the disposition of drugs

targeted for indications of the central nervous system: evaluation using the Mdr1a/Mdr1b knockout mouse model. *Drug Metab. Dispos.* 33, 165–174.

Gao, L., Xia, L., Zhao, F.L., Li, S.C., 2012. Clinical efficacy and safety of the newer antiepileptic drugs as adjunctive treatment in adults with refractory partial-onset epilepsy: A meta-analysis of randomized placebo-controlled trials. *Epilepsy Res.* 103, 31-44.

Hartz, A.M., Bauer, B., 2010. Regulation of ABC transporters at the blood-brain barrier: new targets for CNS therapy. *Mol. Interv.* 10, 293-304.

Kwan, P., Arzimanoglou, A., Berg, A.T., Brodie, M.J., Allen Hauser, W., Mathern, G., Moshe, S.L., Perucca, E., Wiebe, S., French, J., 2010. Definition of drug resistant epilepsy: consensus proposal by the ad hoc Task Force of the ILAE Commission on Therapeutic Strategies. *Epilepsia* 51, 1069-1077.

Kwan, P., Schachter, S.C., Brodie, M.J., 2011. Drug-resistant epilepsy. *N. Engl. J. Med.* 365, 919-926.

Lagas, J.S., Vlaming, M.L., Schinkel, A.H., 2009. Pharmacokinetic assessment of multiple ATP-binding cassette transporters: the power of combination knockout mice. *Mol. Interv.* 9,

136-145.

Löscher, W., Potschka, H., 2005. Blood-brain barrier active efflux transporters: ATP-binding cassette gene family. *NeuroRx*. 2, 86-98.

Löscher, W., Luna-Tortós, C., Römermann, K., Fedrowitz, M., 2011. Do ATP-binding cassette transporters cause pharmacoresistance in epilepsy? Problems and approaches in determining which antiepileptic drugs are affected. *Curr Pharm Des*. 17, 2808-2828.

Owen, A., Pirmohamed, M., Tettey, J.N., Morgan, P., Chadwick, D., Park, B.K., 2001. Carbamazepine is not a substrate for P-glycoprotein. *Br. J. Clin. Pharmacol*. 51, 345-349.

Potschka, H., Fedrowitz, M., Löscher, W., 2002. P-Glycoprotein-mediated efflux of phenobarbital, lamotrigine, and felbamate at the blood-brain barrier: evidence from microdialysis experiments in rats. *Neurosci. Lett*. 327, 173-176.

Potschka, H., Fedrowitz, M., Löscher, W., 2003. Multidrug resistance protein MRP2 contributes to blood-brain barrier function and restricts antiepileptic drug activity. *J. Pharmacol. Exp. Ther*. 306, 124-131.

Rizzi, M., Caccia, S., Guiso, G., Richichi, C., Gorter, J.A., Aronica, E., Aliprandi, M., Bagnati, R., Fanelli, R., D'Incalci, M., Samanin, R., Vezzani, A., 2002. Limbic seizures induce P-glycoprotein in rodent brain: functional implications for pharmacoresistance. *J. Neurosci.* 22, 5833-5839.

Shibata, M., Hashi, S., Nakanishi, H., Masuda, S., Katsura, T., Yano, I., 2012. Detection of 22 antiepileptic drugs by ultra-performance liquid chromatography coupled with tandem mass spectrometry applicable to routine therapeutic drug monitoring. *Biomed. Chromatogr.* 26, 1519-1528.

Sills, G.J., Kwan, P., Butler, E., de Lange, E.C., van den Berg, D.J., Brodie, MJ., 2002. P-glycoprotein-mediated efflux of antiepileptic drugs: preliminary studies in *mdr1a* knockout mice. *Epilepsy Behav.* 3, 427-432.

Uchida, Y., Ohtsuki, S., Katsukura, Y., Ikeda, C., Suzuki, T., Kamiie, J., Terasaki, T., 2011. Quantitative targeted absolute proteomics of human blood-brain barrier transporters and receptors. *J. Neurochem.* 117, 333-345.

van Vliet, E.A., Redeker, S., Aronica, E., Edelbroek, P.M., Gorter, J.A., 2005. Expression of multidrug transporters MRP1, MRP2, and BCRP shortly after status epilepticus, during the latent

period, and in chronic epileptic rats. *Epilepsia* 46, 1569-1580.

Zhang, C., Kwan, P., Zuo, Z., Baum, L., 2012. The transport of antiepileptic drugs by

P-glycoprotein. *Adv. Drug. Deliv. Rev.* 64, 930-942.

Figure legends

Fig. 1. Chemical structures of the 12 antiepileptic drugs.

Fig. 2. The plasma concentration profiles of the 12 antiepileptic drugs in wild-type and *Mdr1a/1b*(-/-) mice. Each point represents the mean \pm S.E. ($n = 4-6$). The plasma concentrations in *Mdr1a/1b*(-/-) mice (filled circle) were compared with those in wild-type mice (open circle) by using repeated measures ANOVA.

Fig. 3. The plasma concentration profiles of the 12 antiepileptic drugs in wild-type and *Mdr1a/1b*(-/-)/*Bcrp*(-/-) mice. Each point represents the mean \pm S.E. ($n = 5-6$). The plasma concentrations in *Mdr1a/1b*(-/-)/*Bcrp*(-/-) mice (filled circle) were compared with those in wild-type mice (open circle) by using repeated measures ANOVA, * $P < 0.05$, ** $P < 0.01$, *** $P < 0.005$.

Fig. 4. Changes in the brain-to-plasma concentration ratio ($K_{p_{\text{brain}}}$) values for the 12 antiepileptic drugs in wild-type, *Mdr1a/1b*(-/-), and *Mdr1a/1b*(-/-)/*Bcrp*(-/-) mice at 60 min after administration. Each bar represents the mean \pm S.E. ($n = 5-11$). Each $K_{p_{\text{brain}}}$ value in the knockout mice was divided by the mean $K_{p_{\text{brain}}}$ value of the corresponding control (wild-type mice). The mean \pm S.E. value of the wild-type mice ($n = 10-11$) were as follows: phenobarbital, 0.734 ± 0.109 ; phenytoin, 0.371 ± 0.026 ; ethosuximide, 0.798 ± 0.065 ; carbamazepine, 0.748 ± 0.042 ; valproic acid, 0.181 ± 0.012 ; clobazam, 0.866 ± 0.047 ; zonisamide, 1.12 ± 0.04 ; lamotrigine, 0.690 ± 0.045 ; gabapentin,

0.432 ± 0.050; topiramate, 0.585 ± 0.023; tiagabine, 0.681 ± 0.047; and levetiracetam, 0.495 ± 0.045. Statistical analyses were performed using ANOVA followed by the Bonferroni test, *P < 0.05, **P < 0.01, ***P < 0.005.

Fig. 5. The relationship between the molecular weight (MW) and brain, kidney or liver-to-plasma concentration ratio ($K_{p_{\text{brain}}}$, $K_{p_{\text{kidney}}}$, or $K_{p_{\text{liver}}}$) values of the 12 antiepileptic drugs in wild-type and *Mdr1a/1b(-)/Bcrp(-)* mice. The observed $K_{p_{\text{brain}}}$, $K_{p_{\text{kidney}}}$, and $K_{p_{\text{liver}}}$ values in the wild-type mice (open circle) and *Mdr1a/1b(-)/Bcrp(-)* mice (filled circle) are shown as the mean values (n = 5–6). A: The solid line represents the final model for the $K_{p_{\text{brain}}}$ value in *Mdr1a/1b(-)/Bcrp(-)* mice: $K_{p_{\text{brain}}}(\text{Mdr1a/1b(-)/Bcrp(-) mice}) = 0.00304 \times \text{MW}$, $r^2 = 0.457$, $P < 0.0001$, and the dashed line represents the correlation between the $K_{p_{\text{brain}}}$ value and MW in wild-type mice: $K_{p_{\text{brain}}}(\text{wild-type mice}) = 0.000837 \times \text{MW} + 0.356$, $r^2 = 0.0706$, $P = 0.404$. B: The solid line represents the correlation between the $K_{p_{\text{kidney}}}$ value and MW in *Mdr1a/1b(-)/Bcrp(-)* mice: $K_{p_{\text{kidney}}}(\text{Mdr1a/1b(-)/Bcrp(-) mice}) = -0.00139 \times \text{MW} + 1.81$, $r^2 = 0.0239$, $P = 0.631$, and the dashed line represents the correlation between the $K_{p_{\text{kidney}}}$ and MW in wild-type mice: $K_{p_{\text{kidney}}}(\text{wild-type mice}) = -0.00386 \times \text{MW} + 2.48$, $r^2 = 0.0493$, $P = 0.488$. C: The solid line represents the correlation between the $K_{p_{\text{liver}}}$ value and MW in *Mdr1a/1b(-)/Bcrp(-)* mice: $K_{p_{\text{liver}}}(\text{Mdr1a/1b(-)/Bcrp(-) mice}) = 0.00524 \times \text{MW}$, $r^2 = 0.617$, $P < 0.0001$, and the dashed line represents the correlation between $K_{p_{\text{liver}}}$ and MW in wild-type mice: $K_{p_{\text{liver}}}(\text{wild-type mice}) = 0.00484 \times \text{MW}$, $r^2 = 0.573$, $P < 0.0001$.

PB: phenobarbital, PHT: phenytoin, ESM: ethosuximide, CBZ: carbamazepine, VPA: valproic acid,
CLB: clobazam, ZNS: zonisamide, LTG: lamotrigine, GBP: gabapentin, TPM: topiramate, TGB:
tiagabine, LVT: levetiracetam

Table 1 Pharmacokinetic parameters, Kp_{kidney}, and Kp_{liver} of 12 AEDs in wild-type and *Mdr1a/1b*(-/-) mice

	CL (mL/min/kg)		V _{ss} (mL/kg)		T _{1/2} (min)		Kp _{kidney}		Kp _{liver}	
	Wild-type	<i>Mdr1a/1b</i> (-/-)	Wild-type	<i>Mdr1a/1b</i> (-/-)	Wild-type	<i>Mdr1a/1b</i> (-/-)	Wild-type	<i>Mdr1a/1b</i> (-/-)	Wild-type	<i>Mdr1a/1b</i> (-/-)
Phenobarbital	3.83 ± 0.60	4.25 ± 1.16	625 ± 36	634 ± 27	142 ± 40	248 ± 146	1.23 ± 0.06	1.20 ± 0.15	1.48 ± 0.19	1.56 ± 0.061
Phenytoin	3.86 ± 0.48	2.98 ± 0.84	1063 ± 62	1136 ± 16	209 ± 43	396 ± 179	0.693 ± 0.040	0.749 ± 0.049	1.39 ± 0.15	1.25 ± 0.10
Ethosuximide	2.99 ± 0.63	3.24 ± 0.74	555 ± 45	568 ± 47	159 ± 34	172 ± 56	0.915 ± 0.050	1.01 ± 0.11	0.934 ± 0.113	0.960 ± 0.083
Carbamazepine	8.16 ± 0.88	8.33 ± 0.83	1482 ± 65	1602 ± 48	136 ± 19	141 ± 15	1.27 ± 0.05	1.38 ± 0.07	1.98 ± 0.10	1.81 ± 0.04
Valproic acid	2.83 ± 0.43	3.25 ± 0.60	375 ± 10	375 ± 18	108 ± 22	97 ± 20	2.24 ± 0.36	1.21 ± 0.16*	0.899 ± 0.057	0.937 ± 0.091
Clobazam	44.4 ± 2.5	45.2 ± 3.0	1752 ± 80	1837 ± 94	29.5 ± 1.4	29.5 ± 0.9	1.37 ± 0.19	1.88 ± 0.10*	2.05 ± 0.09	1.96 ± 0.14
Zonisamide	5.54 ± 0.46	5.71 ± 0.87	1136 ± 74	1130 ± 93	145 ± 10	147 ± 16	1.70 ± 0.07	1.64 ± 0.10	n.d.	
Lamotrigine	5.04 ± 0.38	5.42 ± 0.59	1266 ± 49	1324 ± 32	200 ± 28	187 ± 25	1.94 ± 0.06	2.15 ± 0.14	1.69 ± 0.12	1.57 ± 0.05
Gabapentin	12.6 ± 2.1	9.15 ± 2.06	802 ± 42	845 ± 54	52.5 ± 11.9	84.1 ± 23.5	5.29 ± 1.14	4.29 ± 0.27	1.12 ± 0.03	1.00 ± 0.02**
Topiramate	4.67 ± 0.77	4.22 ± 0.41	846 ± 41	875 ± 17	144 ± 32	152 ± 16	1.21 ± 0.04	1.23 ± 0.04	1.18 ± 0.04	1.12 ± 0.02
Tiagabine	17.5 ± 0.7	18.3 ± 1.7	1308 ± 53	1305 ± 75	52.4 ± 1.0	51.0 ± 3.4	0.602 ± 0.136	0.969 ± 0.171	2.36 ± 0.25	2.26 ± 0.33
Levetiracetam	4.04 ± 0.91	3.10 ± 0.75	658 ± 23	696 ± 21	136 ± 37	216 ± 66	1.31 ± 0.15	1.28 ± 0.04	0.825 ± 0.078	0.806 ± 0.034

Each value represents the mean ± S.E. for 5 or 6 mice.

CL: clearance, V_{ss}: volume of distribution at steady state, T_{1/2} : terminal half-life,

Kp_{kidney}: kidney-to-plasma concentration ratio, Kp_{liver}: liver-to-plasma concentration ratio

*P < 0.05, **P < 0.01, n.d.: not detected

Table 2 Pharmacokinetic parameters, K_p_{kidney}, and K_p_{liver} of 12 AEDs in wild-type and *Mdr1a/1b(-)/Bcrp(-)* mice

	CL (mL/min/kg)		V _{ss} (mL/kg)		T _{1/2} (min)		K _p _{kidney}		K _p _{liver}	
	Wild-type	<i>Mdr1a/1b(-)/Bcrp(-)</i>	Wild-type	<i>Mdr1a/1b(-)/Bcrp(-)</i>	Wild-type	<i>Mdr1a/1b(-)/Bcrp(-)</i>	Wild-type	<i>Mdr1a/1b(-)/Bcrp(-)</i>	Wild-type	<i>Mdr1a/1b(-)/Bcrp(-)</i>
Phenobarbital	2.42 ± 0.78	3.22 ± 1.57	720 ± 65	763 ± 30	1001 ± 858	564 ± 356	1.36 ± 0.19	1.41 ± 0.16	1.44 ± 0.21	1.39 ± 0.11
Phenytoin	4.80 ± 0.70	3.82 ± 0.74	901 ± 26	1008 ± 20*	141 ± 19	218 ± 54	0.558 ± 0.028	0.694 ± 0.052*	1.03 ± 0.07	1.16 ± 0.10
Ethosuximide	3.06 ± 0.59	3.44 ± 1.06	681 ± 50	720 ± 57	196 ± 61	196 ± 62	1.14 ± 0.05	0.956 ± 0.18	0.789 ± 0.101	0.904 ± 0.139
Carbamazepine	6.48 ± 1.23	6.00 ± 0.68	1403 ± 55	1441 ± 43	169 ± 27	172 ± 15	0.734 ± 0.046	1.07 ± 0.06**	1.39 ± 0.08	1.49 ± 0.11
Valproic acid	3.79 ± 0.34	4.38 ± 0.86	391 ± 22	412 ± 23	75.3 ± 11.5	93.1 ± 39.0	1.28 ± 0.11	1.67 ± 0.27	0.909 ± 0.031	0.967 ± 0.107
Clobazam	39.7 ± 1.9	38.9 ± 9.4	1925 ± 97	2212 ± 48*	35.7 ± 2.7	117 ± 83	1.57 ± 0.10	1.69 ± 0.06	1.67 ± 0.10	1.85 ± 0.11
Zonisamide	3.20 ± 0.32	7.45 ± 1.89**	1139 ± 32	1105 ± 30	259 ± 27	122 ± 21**	1.69 ± 0.06	1.68 ± 0.03	n. d.	
Lamotrigine	5.82 ± 0.35	6.42 ± 0.45	1026 ± 40	1149 ± 8	124 ± 9	126 ± 9	1.76 ± 0.12	1.90 ± 0.05	1.09 ± 0.03	1.29 ± 0.09*
Gabapentin	4.14 ± 0.79	9.06 ± 1.75*	610 ± 46	720 ± 58	118 ± 22	74.1 ± 20.1	5.52 ± 0.72	3.27 ± 0.35*	0.941 ± 0.016	0.943 ± 0.024
Topiramate	4.30 ± 0.37	4.57 ± 0.28	735 ± 26	817 ± 19*	123 ± 12	126 ± 8	1.12 ± 0.03	1.20 ± 0.02*	1.14 ± 0.05	1.18 ± 0.02
Tiagabine	11.9 ± 0.7	15.5 ± 2.6	1382 ± 83	1563 ± 72	82.2 ± 7.8	83.2 ± 22.8	1.29 ± 0.10	1.39 ± 0.08	1.89 ± 0.17	2.11 ± 0.15
Levetiracetam	1.57 ± 0.21	3.48 ± 0.53*	477 ± 18	543 ± 19*	230 ± 36	124 ± 26*	0.795 ± 0.045	0.931 ± 0.066	0.636 ± 0.023	0.633 ± 0.006

Each value represents the mean ± S.E. for 5 or 6 mice.

CL: clearance, V_{ss}: volume of distribution at steady state, T_{1/2}: terminal half-life,

K_p_{kidney}: kidney-to-plasma concentration ratio, K_p_{liver}: liver-to-plasma concentration ratio

*P < 0.05, **P < 0.01, n.d.: not detected

Fig. 1

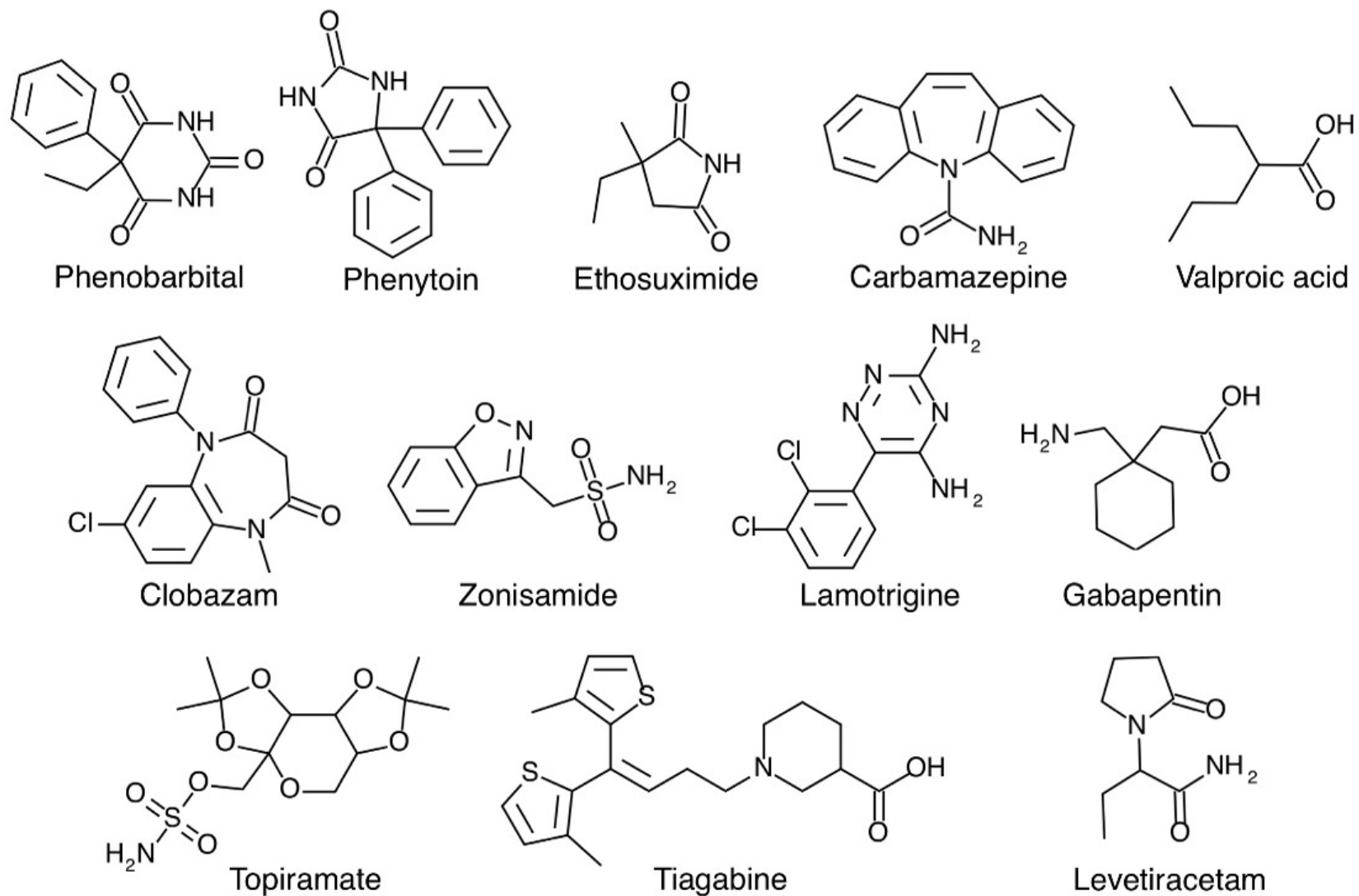


Fig. 2

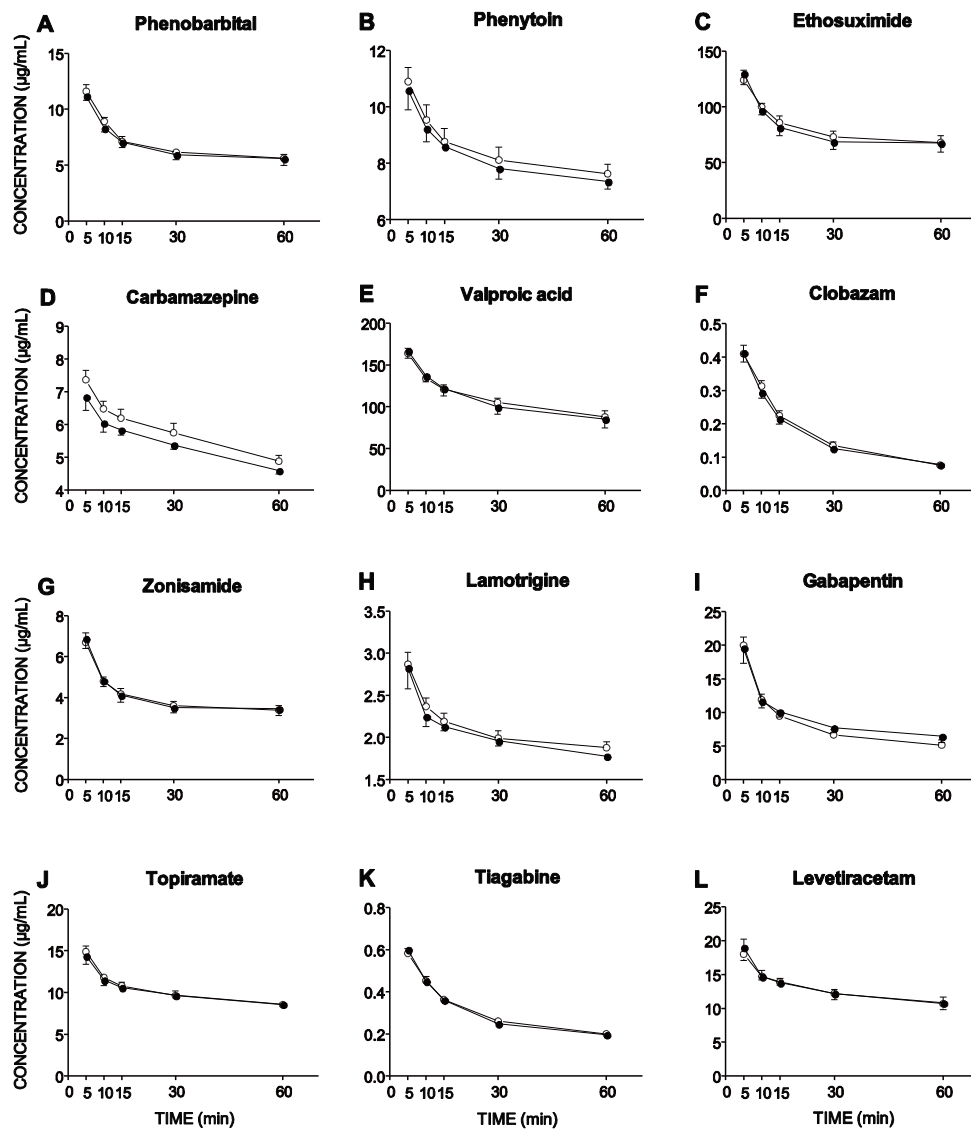


Fig. 3

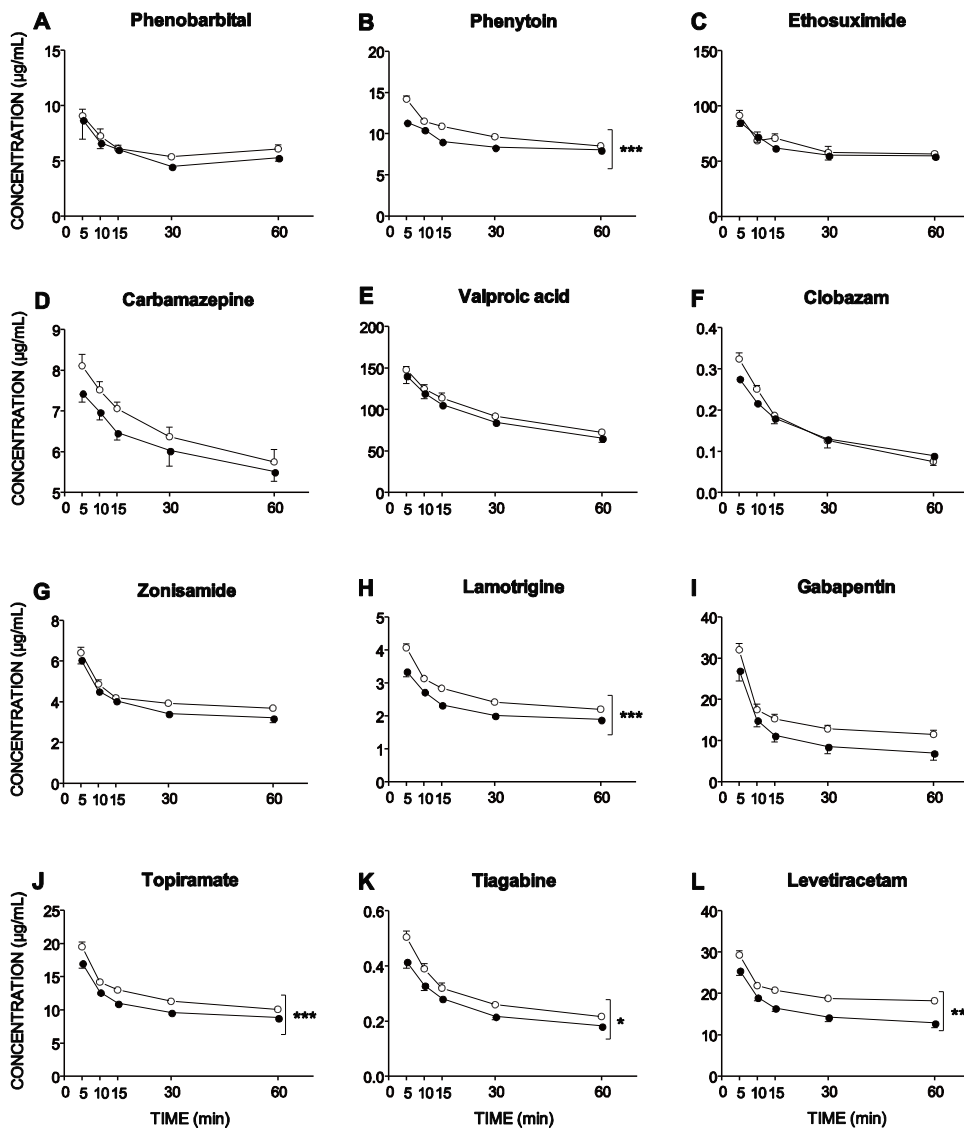


Fig. 4

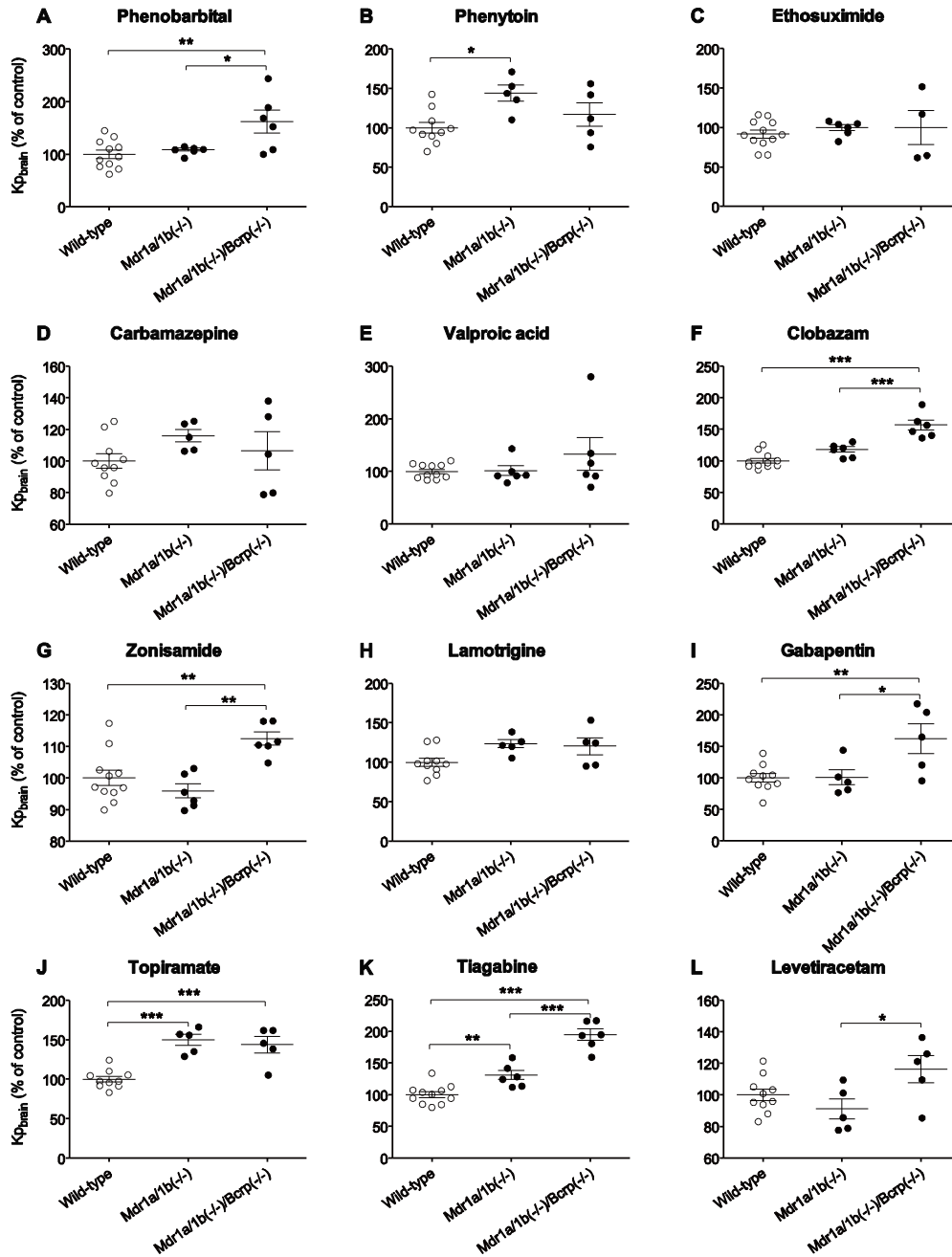


Fig. 5

